Supplementary Information

Designing fluorinated interphase for rechargeable aqueous Al batteries

Zihang Xi,[a] Lianqiang Peng,[a] Jie Zhang,[a] Zhenyu Fan,[a] Xiaotian Wang,[a] Jichi Yang[a] and Qing Zhao,*[a.b]

[a]State Key Laboratory of Advanced Chemical Power Sources, Frontiers Science Center for New Organic Matter, Key Laboratory of Advanced Energy Materials Chemistry (Ministry of Education), College of Chemistry, Nankai University, Tianjin, 300071, China.

[b]Haihe Laboratory of Sustainable Chemical Transformations, Tianjin, 300192, China

Experimental section

Preparation of FAl anodes

Aluminum foils (Al, 0.1 mm thick, 99.99%, LANLIKE) were cleaned by anhydrous EtOH and deionized water. For direct acid treatment, Al foils were immersed in 0.5 m trifluoroacetic acid (HTFA, 99.5%, Macklin) for 0.5 hour. Al foils were placed in 70 °C deionized water for 3 hours (named as HAl). Subsequently, HAl foils were immersed in 0.1m, 0.5 m, 1 m HTFA for 0.5 hour and 1 hour. Then, the acid treated foils were washed three time with deionized water and dried at room temperature to obtain FAl. The side of treated Al foils that contacts with the battery cap was polished off by sandpapers (5000-mesh, Solomen) to enhance the electronic conductivity.

Preparation of Al batteries

The 2032-type coin cells assembled in ambient atmosphere were used for electrochemical measurements. The PTO cathodes were fabricated by mixing pyrene-4,5,9,10-tetraone (PTO, 97%, Energy Chemical), Ketjen black (KB, Guangdong Canrd New Energy Technology Co. Ltd), and polytetrafluoroethylene (PTFE, Heowns) binder in a mass ratio of 4:5:1. Then the mixture was ground and pressed to Ti mesh with the aid of anhydrous EtOH. The cathodes were dried at 60 °C in vacuum before usage with an average mass loading of approximately 1 mg cm^{-2}. Glass fiber (GF/D, Whatman), and 2m $Al(OTF)_3$ (98%, Aladdin) aqueous solutions (100 μL per cell) were used as separators and electrolytes. Ti foils (0.01 mm, Lanlike) were placed on both cathodes and anode side to avoid the corrosion of stainless-steel cells cases.

Electrochemical measurements

The electrochemical measurements were performed using electrochemical workstation (CHI 760E) and battery test system (LAND CT2001A) at ambient atmosphere. Tafel polarization measurements were performed in a three-electrodes configuration where different Al foils were used as working electrodes, Pt was used as counter electrode, and Ag/AgCl (0.222 V vs SHE) was used as reference electrode at a scan rate of 1 mV s^{-1}. EIS was conducted on open current voltage over a frequency range of 10^5 to 10^{-2} Hz with an applied AC amplitude of 5 mV. Al||Al symmetric cells were measured with 2m $Al(OTF)_3$ and 4m $Al(OTF)_3$ electrolytes. Al||PTO full cells were measured with 2m $Al(OTF)_3$ electrolytes.. The voltage region of Al||PTO full cells is from 0.1 to 1.2 V.

Material characterizations

The morphology and elemental distribution of Al anodes and PTO cathodes were characterized by field-emission scanning electron microscopy (SEM, JSM-7900F, JEOL). The microstructural and crystallographic characterizations

of FAl anodes were measured by scanning transmission electron microscopy (STEM; Talos F200X, FEI) including high-resolution transmission electron microscope (HRTEM) images, selected area electron diffraction (SAED), high-angle annular dark field (HAADF) images, and energy dispersive X-ray spectroscopy (EDS) analysis. The XRD patterns of FAl anodes was characterized by X-ray diffractometer (SmartLab, Rigaku) with Cu Kα radiation as the excitation source. X-ray photoelectron spectroscopy (XPS) of FAl anodes and PTO cathodes was conducted by an X-ray photoelectron spectrometer (Escalab 250Xi, Thermo Fisher Scientific). Raman spectra of FAl anodes were obtained on a spectrometer (inVia Qontor, Renishaw) with 532 nm excitation wavelength. Infrared spectra of FAl and PTO electrodes were collected by a Fourier Transform Infrared spectrometer (FTIR, TENSOR II, Bruker). The ^{1}H NMR spectra of PTO cathodes was performed by NMR spectrometer (AVANCE III 400MHz, Bruker). The samples were dissolved in DMSO-d6 (99.8%, J&K Scientific) and filtered before NMR measurement. ^{1}H NMR result for PTO: 8.33 (4H),7.74 (2H). ^{1}H NMR result for PTO-2H: 7.79 (2H), 8.18 (2H), 8.47 (2H), 9.45 (2H). For SEM, FTIR, NMR, and XPS characterizations, the PTO cathodes were meticulously rinsed with deionized water to remove residual electrolytes and subsequently vacuum dried at 60 °C.

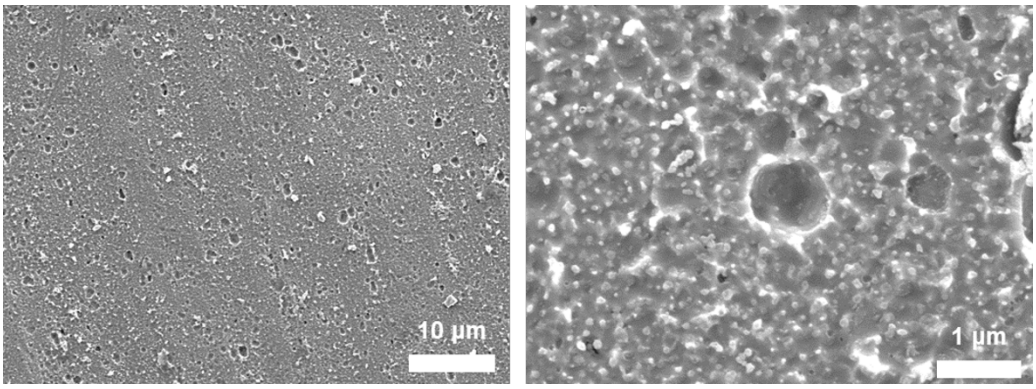

Fig. S1 SEM images of Al foils treated directly by HTFA.

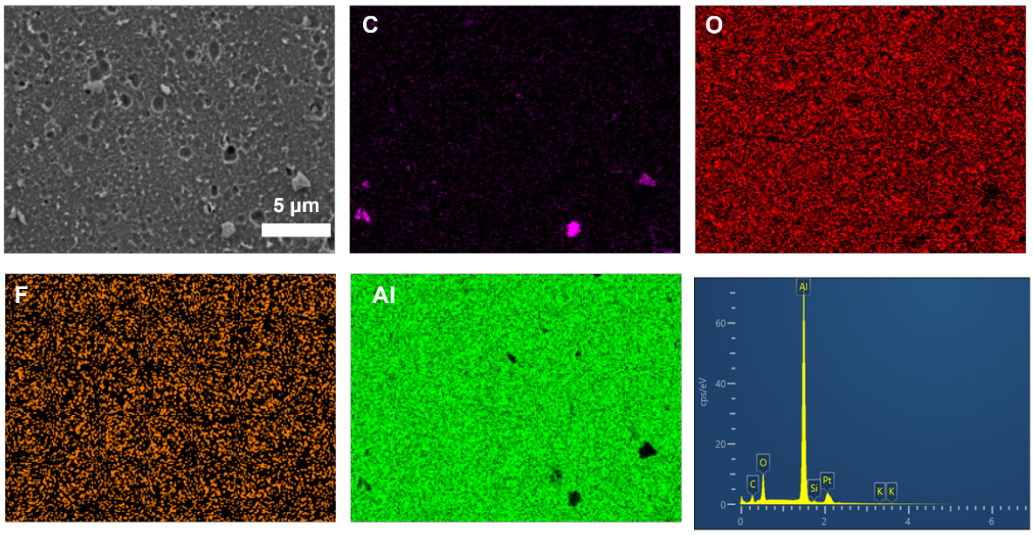

Fig. S2 SEM and corresponding EDS mapping analysis of Al foils treated directly by HTFA.

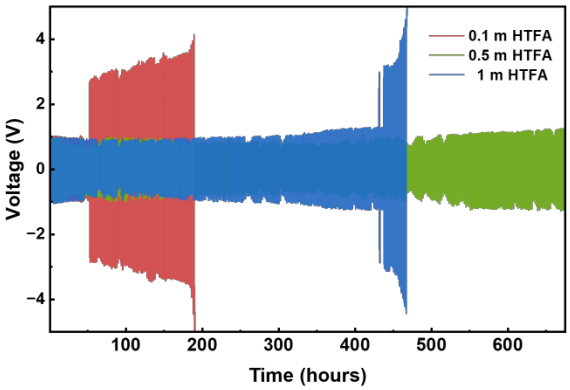

Fig. S3 Cycling performance of symmetric batteries using Al foils anodes treated by different concentrations of HTFA.

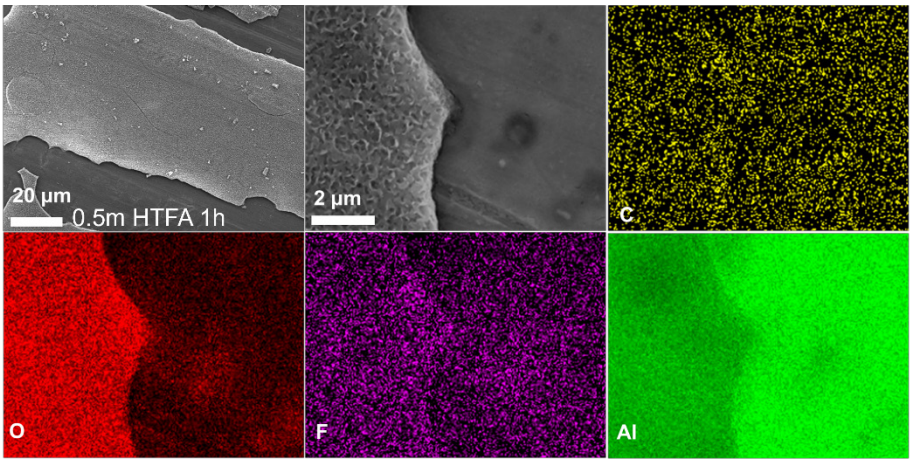

Fig. S4 SEM and corresponding EDS mapping images of Al foils treated by 0.5 m HTFA for 1 h.

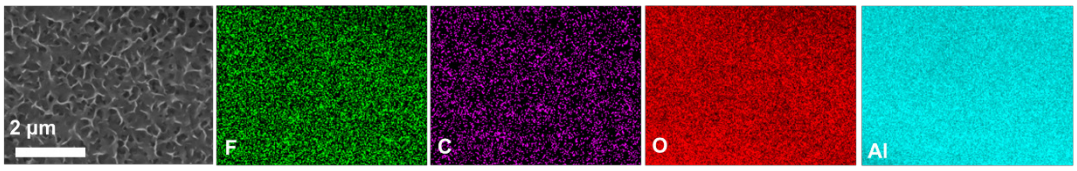

Fig S5. SEM and corresponding EDS mapping images of Al foils treated by 0.5 m HTFA for 0.5 h.

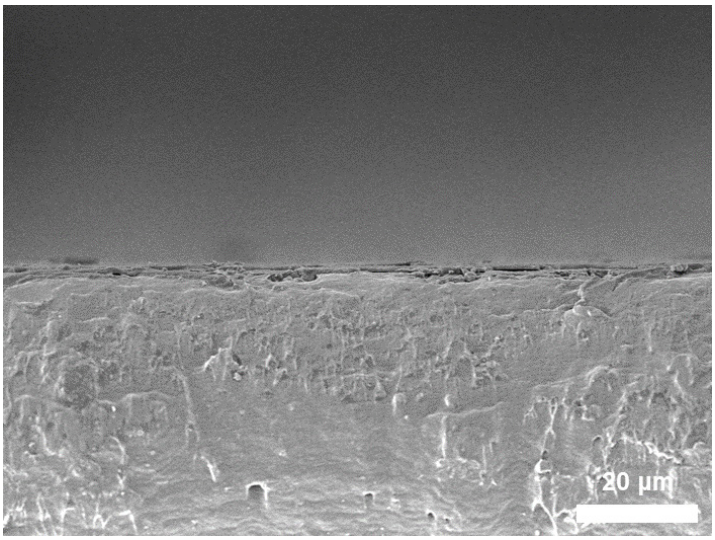

Fig. S6 Cross-sectional SEM image of FAl anode.

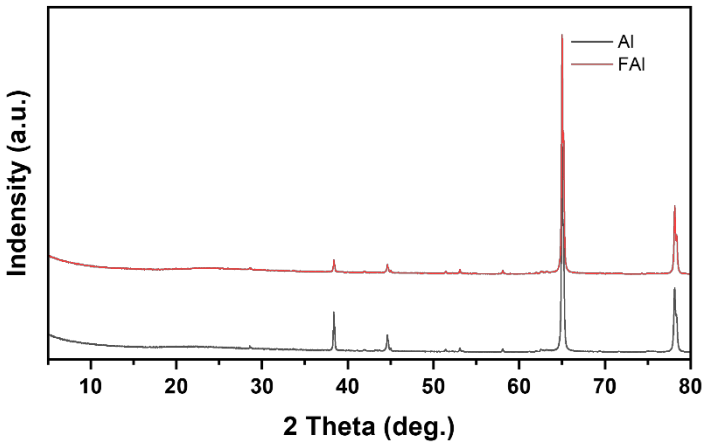

Fig. S7 XRD pattern of pristine Al and FAl anodes.

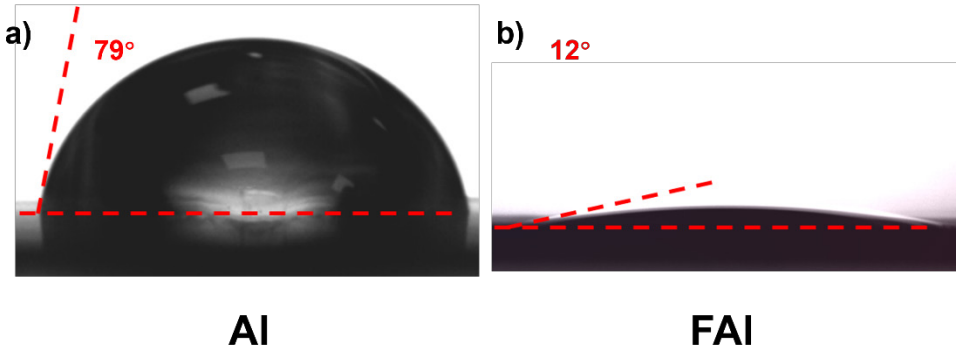

Fig. S8 Contact angle measurements of pristine (a) Al and (b) FAl anodes with 2m $Al(OTF)_3$ electrolyte.

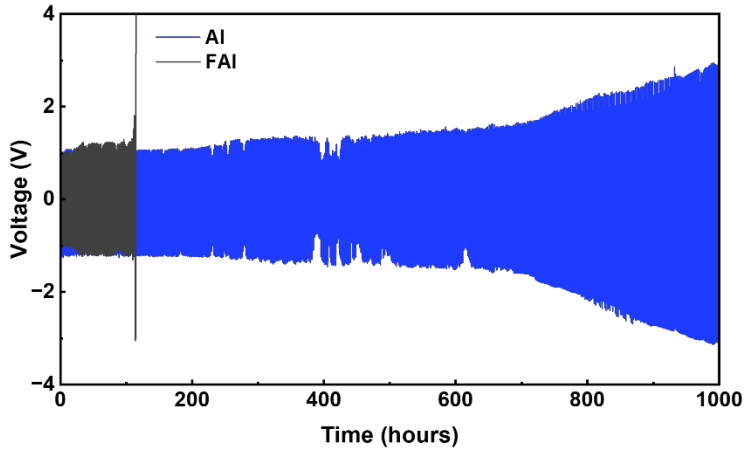

Fig. S9 Cycling performance of symmetric batteries using 2 m $Al(OTF)_3$ electrolytes, pristine Al and FAl anodes at current density of 0.05 mA cm^{-2}.

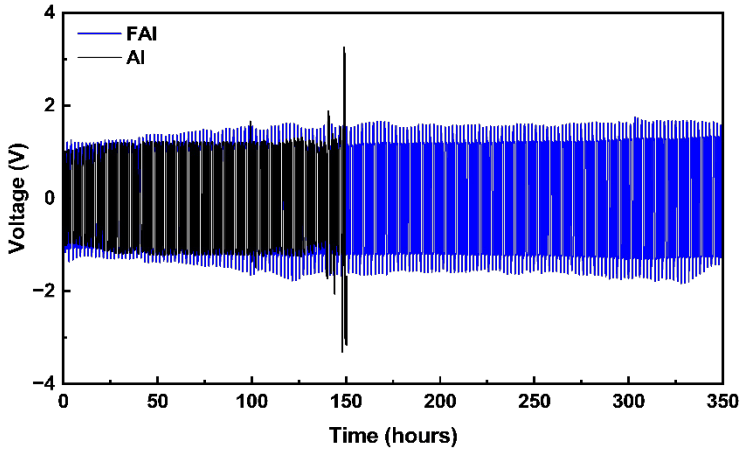

Fig. S10 Cycling performance of symmetric battery using 4 m $Al(OTF)_3$ electrolytes, pristine Al and FAl anodes at current density of 0.05 mA cm^{-2}.

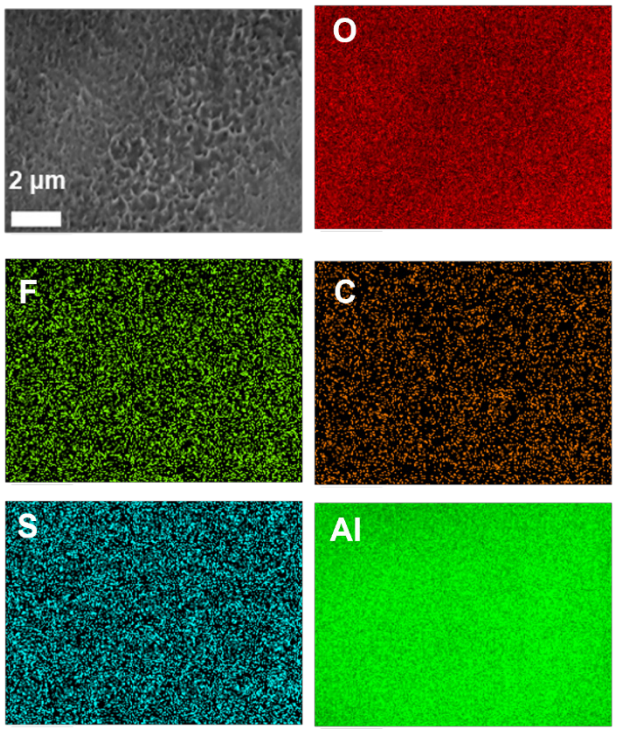

Fig. S11 SEM and corresponding EDS mapping images of FAl anodes after 50 cycles.

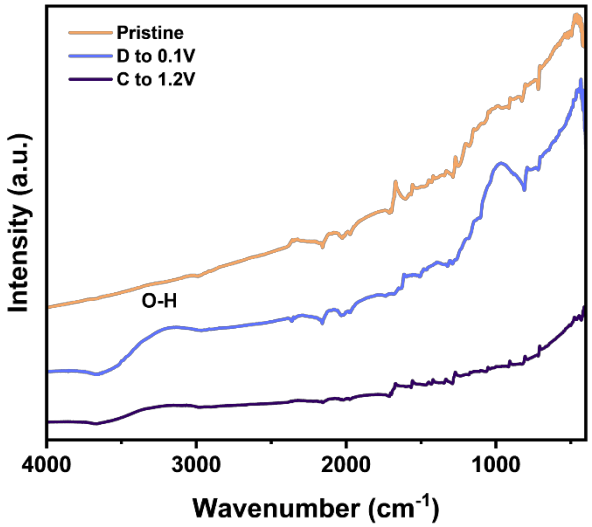

Fig. S12 FTIR spectra of PTO electrodes at different states and 400-4000 cm^{-1} range.

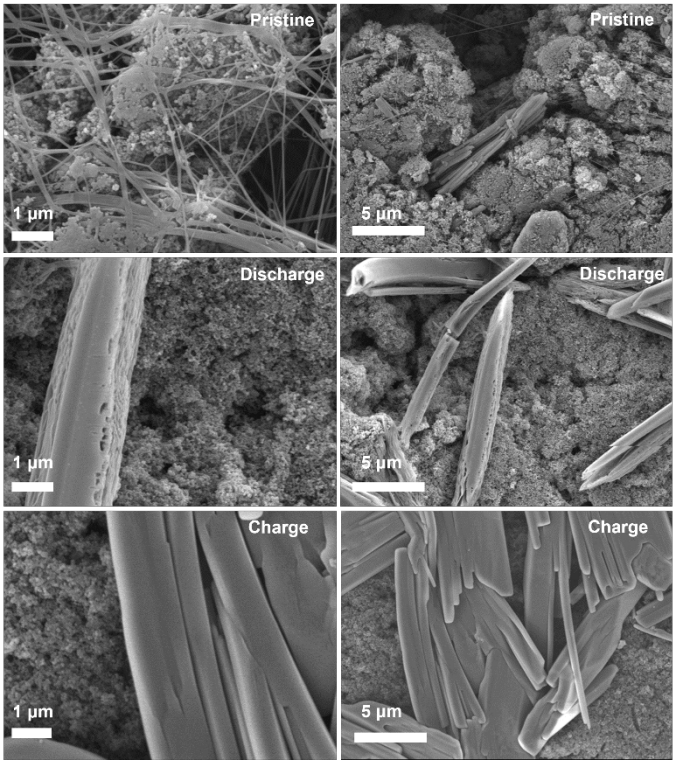

Fig. S13 SEM images of PTO electrodes at different states.

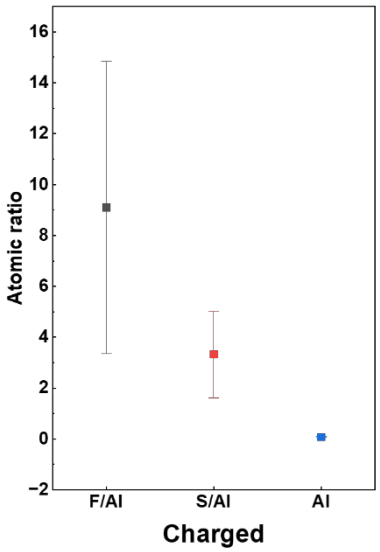

Fig. S14 F/Al, S/Al and Al atomic ratio by SEM-EDS analysis of PTO electrodes at charged state.

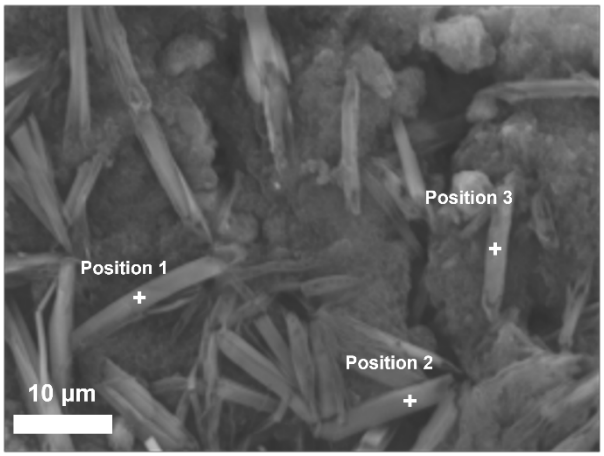

Fig. S15 SEM images and selected positions for EDS measurement of PTO electrodes washed by H_2O and at discharged states.

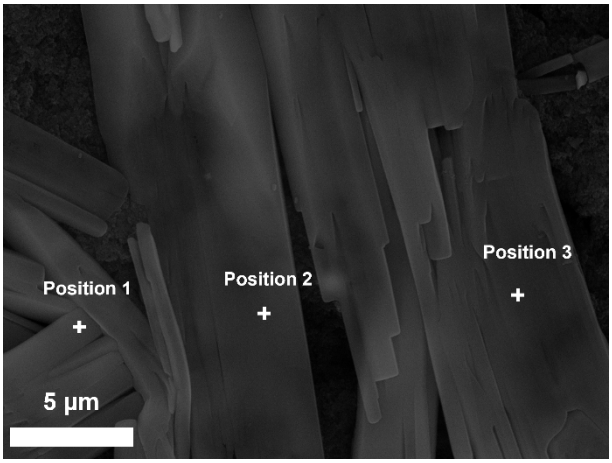

Fig. S16 SEM images and selected positions for EDS studies of PTO electrodes washed by H_2O and at charged states.

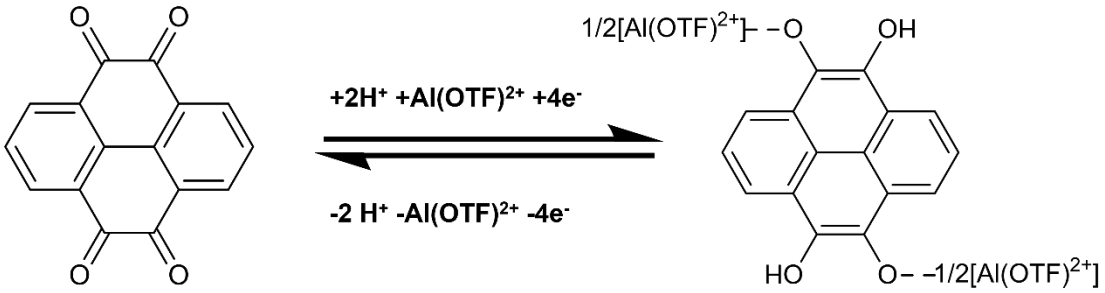

Fig. S17 Proposed mechanism of the charging and discharging process of PTO cathode.

Table S1. Interfacial resistance (R_{int}) of symmetric and full batteries obtained from the equivalent circuit diagram (upper).

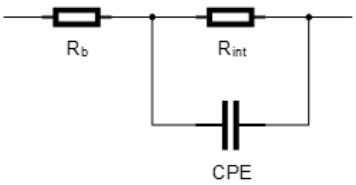

	Al||Al	FAl||FAl	Al||PTO	FAl||PTO
R_{int} (Ω)	33618	7740	14580	2604

Table S2. Comparison of electrochemical performance of symmetric batteries by various anodes processing methods.

Anode	Electrolyte	Current density (mA cm^{-2})	Cycling Stability (hours)	Ref.
TAl	1 m $Al(OTF)_3$	0.2	50	1
Urea-TAl	1 m $Al(OTF)_3$	0.1	180	2
Acm-TAl	1 m $Al(OTF)_3$	0.05	300	3
PVDF-Al	1 m $Al(OTF)_3$	0.1	100	4
Al@a-Al	0.5 m $Al_2(SO_4)_3$	0.05	800	5
Mn/Ti/Zr-Al	1 m $Al(OTF)_3$	0.1	300	6
Sn@Al	0.5 m $Al_2(SO_4)_3$	0.05	900	7
Al/AlPON	1 m $Al(OTF)_3$	1	28	8
FAl	2 m $Al(OTF)_3$	0.05	1000	This work

Table S3. SEM-EDS elements analysis of pristine Al and FAl anodes after 50 cycles.

	At %	
Element	Al	FAl
C	11.8	5.8
O	2.5	41.02
F	0.1	1.37
Al	85.5	51.29
S	0.1	0.52

Table S4. Selected positions EDS elements analysis of PTO electrodes washed by H_2O at discharged/charged states.

	Discharged			charged		
Element	1	2	3	1	2	3
C	85.11	84.45	82.2	83.04	82.82	84.61
O	10.96	12.82	14.81	15.94	16.28	14.37
F	2.69	1.76	2.22	0.77	0.58	0.63
Al	0.58	0.46	0.38	0.07	0.08	0.08
S	0.67	0.51	0.39	0.19	0.24	0.31

References

1. Q. Zhao, M. J. Zachman, W. I. Al Sadat, J. Zheng, L. F. Kourkoutis and L. Archer, *Sci. Adv.*, 2018, **4**, eaau8131.
2. S. Kumar, T. Salim, V. Verma, W. Manalastas and M. Srinivasan, *Chem. Eng. J.*, 2022, **435**, 134742.
3. R. Bai, J. Yang, G. Li, J. Luo and W. Tang, *Energy Storage Mater.*, 2021, **41**, 41–50.
4. Q. Hao, F. Chen, X. Chen, Q. Meng, Y. Qi and N. Li, *Electrochim. Acta*, 2022, **421**, 140495.
5. C. Yan, C. Lv, B.-E. Jia, L. Zhong, X. Cao, X. Guo, H. Liu, W. Xu, D. Liu, L. Yang, J. Liu, H. H. Hng, W. Chen, L. Song, S. Li, Z. Liu, Q. Yan and G. Yu, *J. Am. Chem. Soc.*, 2022, **144**, 11444–11455.
6. Q. Hao, F. Chen, X. Chen, Q. Meng, Y. Qi and N. Li, *ACS Appl. Mater. Interfaces*, 2023, **15**, 34303–34310.
7. B.-E. Jia, E. Hu, Z. Hu, J. J. Liew, Z. Hong, Y. Guo, M. Srinivasan, Q. Zhu, J. Xu, J. Chen, H. Pan and Q. Yan, *Energy Storage Mater.*, 2024, **65**, 103141.
8. L. Tao, Z. Wu, Y. Zhang, R. Szilagyi and J. Liu, *Small*, 2026, **22**, e11148.